Journal of the European Ceramic Society 21 (2001) 2681–2686

www.elsevier.com/locate/jeurceramsoc

Polar grain boundaries in undoped $SrTiO_3$ ceramics

J. Petzelt[a,*], I. Gregora[a], I. Rychetský[a], T. Ostapchuk[a], S. Kamba[a], P. Vaněk[a], Y. Yuzyuk[b,1], A. Almeida[b], M.R. Chavez[b], B. Gorshunov[c,2], M. Dressel[c], S. Hoffmann-Eifert[d], R. Waser[d]

[a]*Institute of Physics, Acad. Sci. CR, Na Slovance 2, 182 21 Praha 8, Czech Republic*
[b]*Departamento de Fisica, IFIMUP, Faculdade de Ciencias da Universidade do Porto, Rua do Campo Alegre 687, 4169-007, Portugal*
[c]*1. Physikalishes Institut, Universtät Stuttgart, D-70550 Stuttgart, Germany*
[d]*Institut f. Festkörperforschung, Forschungszentrum Julich, D-52425 Jülich, Germany*

Abstract

Raman and infra-red spectroscopic investigations of nominally pure $SrTiO_3$ ceramics have revealed a clear presence of polar phase whose manifestation steeply increases on cooling from room temperature. The Raman strengths of the Raman-forbidden infra-red modes are proportional to $\omega_{TO1}^{-\alpha}$ ($\alpha \approx 1.5$) where ω_{TO1} is the polar soft mode frequency. Our explanation is based on an assumption of a temperature independent polarization P_f fixed at grain boundaries. The effective polar soft mode is slightly shifted upwards at low temperatures, becomes broader and strongly coupled with the E_g component of the structural soft mode which shows that P_f is perpendicular to the tetragonal *c*-axis. © 2001 Elsevier Science Ltd. All rights reserved.

Keywords: Dielectric permittivity; Grain boundaries; Polar soft mode; Strontium titanate (STO) ceramics

1. Introduction

Strontium titanate $SrTiO_3$ (STO) has been one of the most popular materials since the discovery of its incipient ferroelectricity and polar soft mode behavior.[1] Owing to its high dielectric permittivity that increases on cooling and to its low microwave (MW) losses it is the most attractive material for many high frequency and MW applications, particularly at low temperatures.[2–4] For this reason, great attention has been paid recently to dielectric properties of STO thin films, which, however, show dramatic differences compared to bulk samples. The permittivity is much smaller and thickness dependent, its increase on cooling saturates at higher temperatures[5–7] and, correspondingly, the polar mode softening levels off at much higher frequencies.[8–11] Several reasons affecting this behavior were discussed: influence of a low permittivity layer on the electrode–film interface,[5,6,12–14] stress caused by the mismatch with the substrate,[14,15] non-stoichiometry, porosity and granularity.[12,14,16] However, so far it has not been clear which of these effects (if any) predominates. To simplify the situation and eliminate all the effects but grain boundaries (and possible point defects), we decided to study bulk STO ceramics.

Unlike single crystals, surprisingly little attention has been so far paid to pure STO ceramics. Earlier literature reports on dielectric data including the MW range[2,3] which show that, like in single crystals, there is no appreciable dielectric dispersion present down to liquid He temperatures up to the 10^{10} Hz range. However, the permittivity values at He temperatures are several times smaller in ceramics (few thousands) than in good single crystals, where they reach nearly 25,000,[17,18] and the MW losses in ceramics are also appreciably higher and grain size dependent.[2,3] No soft mode studies on STO ceramics are known to the authors, even if it is clear (via Lyddane–Sachs–Teller relations) that the lower permittivity should imply a smaller softening of the soft mode. This letter reports on our Raman and IR reflectivity measurements, which not only confirmed this effect, but also presented a clear evidence for existence of polar regions in STO ceramics. Some of our preliminary data have been published recently.[10,19]

2. Experimental

The STO ceramics samples were prepared by a conventional mixed-oxide route.[20] The unstrained, single-

* Corresponding author. Tel.: +420-2-6605-2166; fax: +420-2-86890527.
E-mail address: petzelt@fzu.cz (J. Petzelt).
[1] Permanent address: Faculty of Physics, Rostov State University, Rostov-on-Don, 344090 Russia.
[2] Permanent address: General Physics Institute, RAS, 119991 Moscow, Russia.

0955-2219/01/$ - see front matter © 2001 Elsevier Science Ltd. All rights reserved.
PII: S0955-2219(01)00345-4

phase stoichiometric samples were non-porous (98.8% of theoretical density). The mean grain size of about 1–2 μm was determined from SEM analysis. The impurity content was determined by means of ICP-AES analysis. The concentration of heterovalent impurities (e.g. Al, Fe, K, Na, Nb) was below 150 ppm, homovalent impurities of Ba (320 ppm) and Ca (550 ppm) originate from the precursor powder, contamination with Si (150 ppm), Y (110 ppm) and Zr (2100 ppm) is caused by the milling process. Such an impurity level (particularly Ca) may lead to an increase in low-temperature permittivity in single crystals, but does not change the phase diagram appreciably. The samples were mechanically polished with an alumina slurry and chemically polished with Synthon (fluoride based SiO_2 slurry). Since in the case of STO single crystals it is now well established that the surface treatment plays an important role in the dielectric[5] as well as X-ray and neutron scattering experiments,[23,24] we decided to pay attention to this problem also in the case of ceramics. Some of the samples were etched for about 1 h in the boiling (130 °C) concentrated ortho-phosphoric acid to remove a several μm thin layer from the surface.[5,18]

The standard dielectric measurements revealed a usual dispersionless permittivity values with a monotonous increase on cooling (Curie–Weiss behavior above ~100 K) reaching almost 10,000 at 10 K, which is a higher value than that reported on ceramics.[3] MW measurements at 36.2 GHz performed from 300 to 90 K[19] have revealed the same permittivity values confirming no appreciable dispersion below 10^{10} Hz. The IR reflectivity measurements (20–650 cm^{-1}, 10–300 K) were carried out using Bruker IFS 113v Fourier transform spectrometer equipped with pyroelectric DTGS room temperature detector as well as cooled (1.5 K) Si bolometer. In addition, submillimeter reflectivity (15–25 cm^{-1}, 300–5 K) was also measured using a monochromatic backward-wave-oscillator (BWO) spectrometer. The unpolarized Raman spectra were taken using Ar^+ Coherent INOVA 90 laser and Jobin Yvon T64000 spectrometer with CCD and photon counting detector in a pseudo back-scattering geometry in the 15–300 K range.

3. Results and discussion

In Fig. 1, we show the IR reflectivity including the BWO data. We have revealed that the etched surface yields higher room temperature reflectivity in the 90–150 cm^{-1} range than the polished sample (and even single crystal), which results in lower soft mode damping and absence of the additional overdamped mode below the soft mode response reported by us on the polished ceramics.[10] Because of the surface scattering problem at higher frequencies, in Fig. 1 we combined spectra below 150 cm^{-1} from the etched sample and above 150 cm^{-1} from the polished one. The spectra were fitted in a standard way to a factorized form of the dielectric function[25] to obtain the polar phonon mode parameters. The low-frequency end of the calculated real permittivity agrees well with the dielectric measurements. In Fig. 2, we show the calculated imaginary part ε'' of the dielectric function. In addition to 3 IR active transverse optic modes TO_1 (soft mode), TO_2, and TO_4 clearly seen at room temperature and the E_u mode activated from the *R*-point of the Brillouin zone below the antiferrodistortive transition temperature T_a due to the Brillouin zone folding, an additional mode (denoted by X) not appearing in single crystals arises near 40 cm^{-1} at low temperatures. Also, in contrast to single crystals where $T_a \cong 105$–110 K,[27] in our ceramics $T_a = 132$ K. This shift could be caused by internal stress in our ceramics because the hydrostatic pressure is known to increase T_a by ~20 K/Gpa.[28]

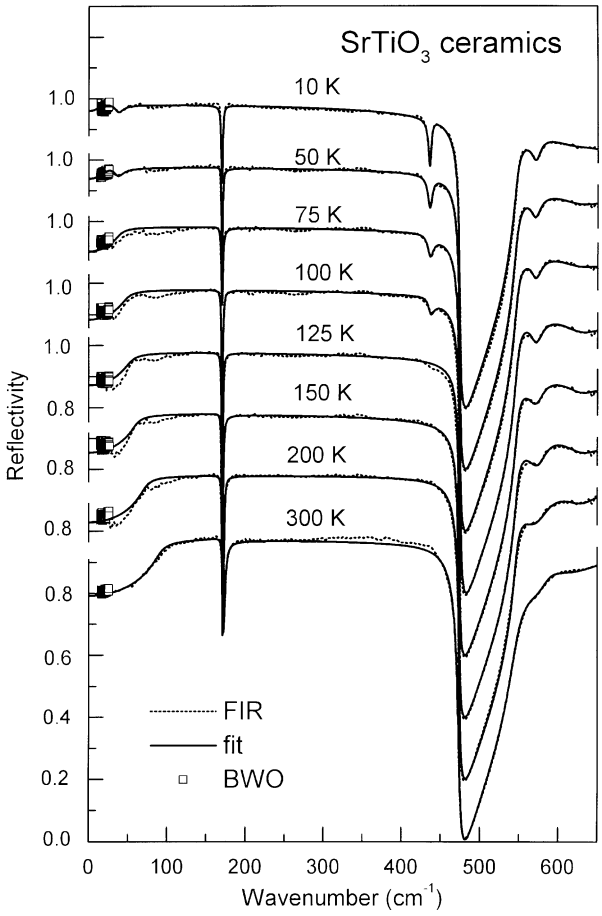

Fig. 1. IR reflectivity of the STO ceramics together with BWO data and multi-oscillator fits (see text) at selected temperatures.

Selected Raman spectra reduced by the temperature factor are shown in Fig. 3. Like in single crystals[21,26,27] the second-order features dominate the spectra at room temperature. On cooling, however, IR-active modes emerge in addition to the folded *R*-point modes. At low temperature, the X mode at 40 cm^{-1} and a heavily damped TO_1 mode, which appears as a central component in

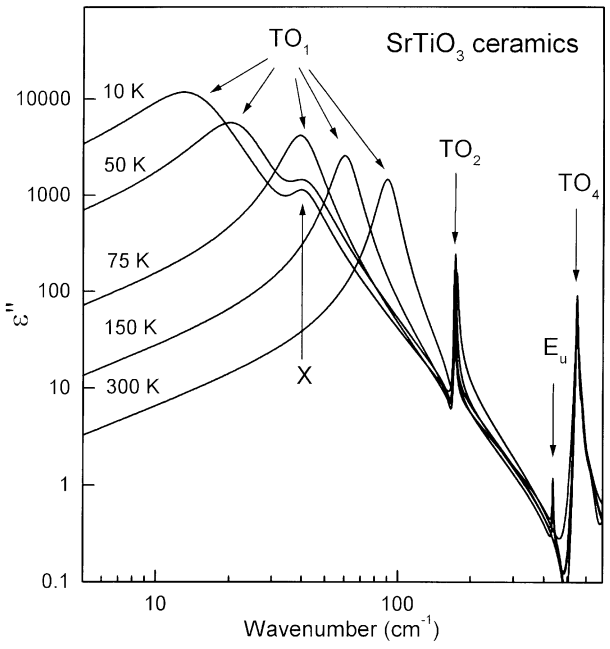

Fig. 2. Dielectric loss spectra calculated from the reflectivity fits.

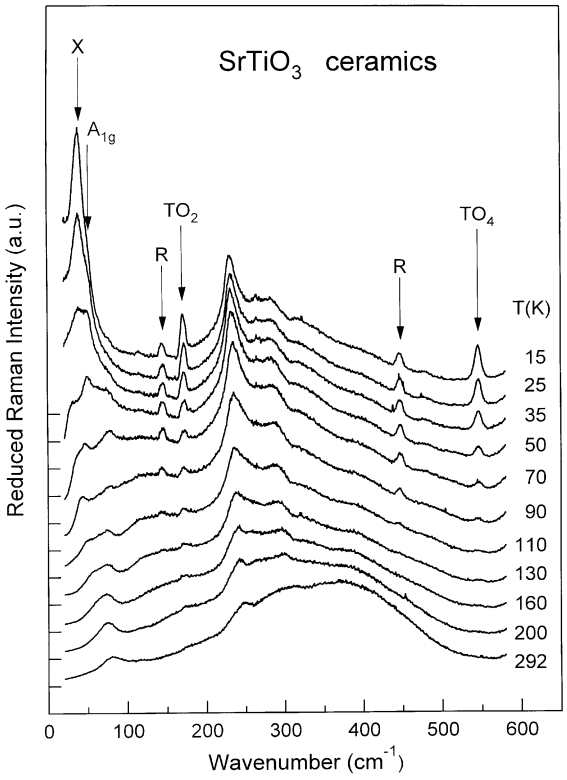

Fig. 3. Reduced unpolarized Raman spectra of STO ceramics at selected temperatures.

non-reduced spectra, dominate the low-frequency range. In Fig. 4, we plotted the temperature dependences of all mode frequencies below 100 cm^{-1} from IR and Raman data carefully fitted by independent multi-oscillator

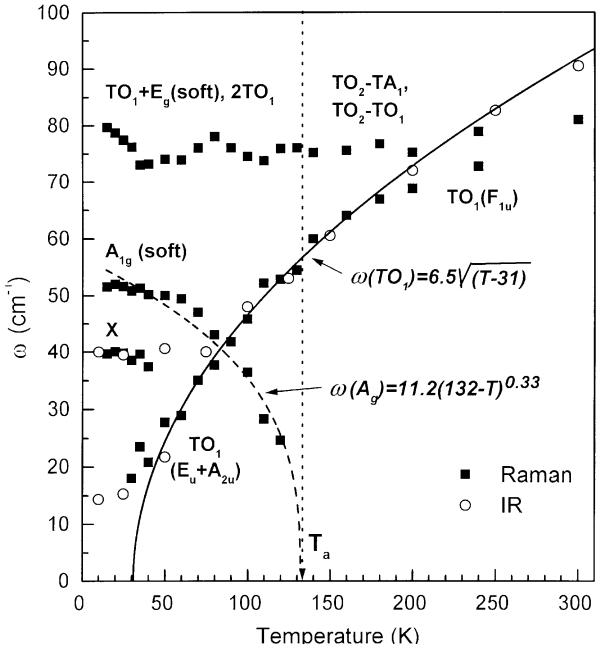

Fig. 4. Temperature dependences of the observed low-frequency mode frequencies together with their assignment—comparison of FIR and Raman data.

model. Like in single crystals, the ω_{TO1} frequency obeys the classical Cochran softening law above $\sim$ 60 K with the extrapolated zero frequency near 31 K (see the full line in Fig. 4). Like in single crystals, the deviation from the Cochran fit at low temperatures is mainly due to the well known quantum zero-point fluctuations. Below T_a the single crystal Raman data display a well-known soft $A_{1g}+E_g$ doublet[27] which saturates at low temperatures near 49 and 15 cm^{-1}, respectively. In our ceramics we see the weak A_{1g} component in agreement with crystal data (our fit yields the saturated value $\sim$ 51 cm^{-1}; see Fig. 4). We assign the X mode to the missing E_g component whose strengthening and partial hardening is caused by a coupling with the TO_1 soft mode. Unfortunately, the limited accuracy of our low-frequency data did not allow us to determine the coupling parameters unambiguously. The temperature dependence of the totally symmetric A_{1g} component shows that the primary order parameter, the TiO_6 octahedra tilt, attains the same spontaneous value like in single crystals. However, the A_{1g}–E_g splitting, which in our case at low temperatures amounts to $\sim$9 cm^{-1} only, measures the secondary order parameter, the tetragonal deformation (neglecting the small E_g frequency renormalization caused by the discussed coupling). As both these quantities are proportional to the order parameter squared,[29,30] it appears that the low-temperature spontaneous tetragonal deformation in our ceramics is by an order of magnitude smaller than that in single crystals. This can be understood as a result of volume clamping of individual grains below T_a.

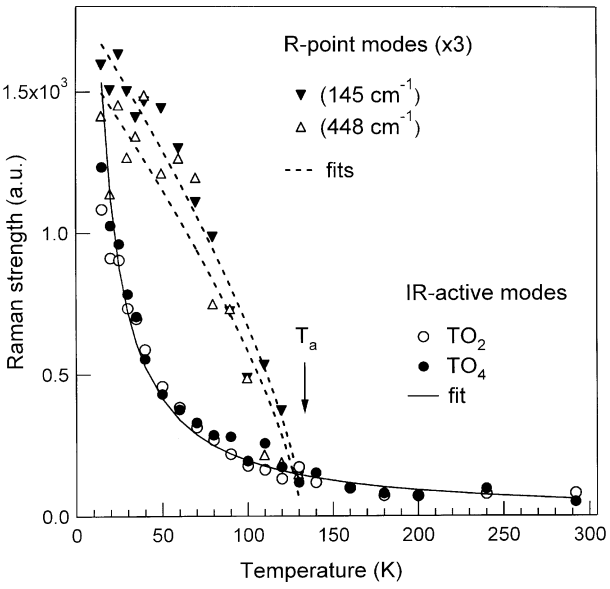

Fig. 5. Raman strengths of the *R*-point modes and IR modes as a function of temperature.

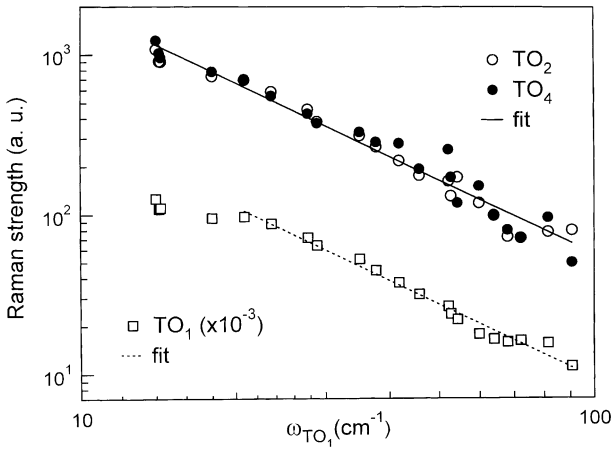

Fig. 6. Raman strengths of the IR modes as a function of the soft mode frequency ω_{TO1}.

The temperature dependences of the Raman strengths (see Fig. 5) of the folded *R*-point modes obey the power law $I_R \propto (T_a - T)^{\gamma}$ with $T_a = 132$ K and $\gamma = 0.72 \pm 0.01$ which agrees well with that observed and theoretically expected in single crystals (γ should be twice the critical index β of the order parameter from symmetry considerations[30]). Unlike the *R*-point modes, the IR modes have nonzero Raman strength even at room temperature already and show a steeper increase on cooling. In view of our further analysis we tried a power law fit to correlate these strengths with the TO_1 frequency. A good fit can be achieved with $I_R \propto \omega_{TO1}^{-\alpha}$, $\alpha = 1.54 \pm 0.06$ as shown in Fig. 6. Also the TO_1 mode strength was estimated by integrating our reduced Raman strength from 20 to 90 cm^{-1}. One can see that, except for temperatures below 50 K, where the soft mode response merges with our unresolved central line, this strength obeys the same law as that of TO_2 and TO_4 modes. The gradual appearance of forbidden polar modes in our Raman spectra manifests the local loss of the inversion center. Similar symmetry breaking, but only at much lower temperatures, was already observed in Ca-doped[21,22] and O[18] isotope exchanged STO single crystals,[31] in thin films[32] and even in nominally pure STO crystals[33] and was assigned to ferroelectric fluctuations. The bilinear coupling of the TO_1 soft mode only to the E_g component (not to the A_{1g} one in the case of our ceramics) requires by symmetry a polar phase with the polarization perpendicular to the tetragonal *c*-axis.

Our explanation is based on an assumption that at grain boundaries a frozen polarization P_f exists independent of temperature. This is a plausible assumption since the recent careful studies of a STO bicrystal have shown that the structure of the grain boundary is well defined, insulating and sufficiently asymmetric to be connected with a dipole moment.[34,35] Another origin of P_f could be in localized point defects, e.g. O vacancies or Ca impurities whose concentration at grain boundaries could be much higher than the average one. Using the Landau–Ginzburg type of approach to calculate inhomogeneous polarization in a small ferroelectric particle,[36] the polarization inside a thin slab can be expressed as

$$P(x) = P_f \frac{\cosh(x/\xi)}{\cosh(D/2\xi)} \approx P_f\left(\exp\left(-\frac{x + D/2}{\xi}\right) + \exp\left(\frac{x - D/2}{\xi}\right)\right) \quad (1)$$

where P_f is the surface polarization, x is the space coordinate normal to the slab ($x = 0$ in the slab center), D its thickness which is much larger than the correlation length ξ of the polarization fall off, and ξ is found to be proportional to ω_{TO1}^{-1}. In our model, the average polarization P_{av} is proportional to ξ, but in general, assuming the inter-defect distances substantially larger than ξ, one can show that $P_{av} \propto \xi^d$ where d is the dimensionality of the polarization propagation from the polar defect (for diluted polar point defects—e.g. grain corners—$d = 3$; for isolated polar linear defects—e. g. grain edges—$d = 2$; for isolated polar surfaces $d = 1$). In our case of finite grains one could expect the main contribution coming from the grain surfaces with $d = 1$, implying that the experimental d should be certainly smaller than 3, or even than 2. The Raman strength of polar modes is obviously proportional to the total volume of polar regions (we assume incoherent scattering of individual grains) or averaged polarization, i.e. also to ξ^d, and our experiment yields $d \approx 1.5$ in agreement with theoretical expectation.

Similar model can be used also to calculate the dielectric response function. The polarization is localized in the

grain boundary layer of the characteristic thickness ξ whose permittivity ε_l is connected with the stiffened soft mode response in these regions, while the grain interior permittivity is that of the single crystal $\varepsilon_{sc}(\omega)$. Then one can use the brick model approach successfully used for the discussion of dielectric properties in the case of $BaTiO_3$ ceramics.[37] In this model the effective dielectric response is estimated like a series combination of the bulk and surface layer capacitances

$$\frac{1}{\varepsilon} = \frac{x}{\varepsilon_{sc}} + \frac{(1-x)g}{\varepsilon_l} \tag{2}$$

where $(1-x) \propto \xi^d$ is the volume fraction of polar grain boundary layers, x is the volume fraction of nonpolar grain interior, and g is a geometrical factor somewhat smaller than unity. Considering both permittivities (dielectric functions) as given by soft oscillators only (for simplicity with the same dampings and strengths in layers like in the bulk), the soft mode frequency ω_{eff} is shifted up to

$$\omega_{eff}^2 = \omega_{sc}^2 + 3\xi\left(g\omega_l^2 - \omega_{sc}^2\right)/D > \omega_{sc}^2, \quad D >> \xi \tag{3}$$

where ω_l, ω_{sc} are TO_1 mode frequencies in the boundary layer and single crystal, respectively. The short-range forces appearing near the grain boundaries and discussed in Ref. 35 in connection with the dynamics of a small ferroelectric particle are neglected in the above model, but their inclusion can be shown to yield qualitatively the same result. Our experiment gives the lowest low-temperature value of ω_{TO1} about 14 cm^{-1} whereas its single domain crystal values are 7.8 and 16.5 cm^{-1} for the split E_u and A_{2u} components, respectively[38] (10.7 cm^{-1} as a weighed average). Our low-temperature TO_1 mode damping is $\sim$12 cm^{-1} compared with much smaller values in single crystals.[8,38] The higher effective soft mode damping could be accounted for by averaging over the anisotropy and distribution of grain shapes and sizes.

The hybridization of the TO_1 with the E_g mode (X-mode) due to symmetry lowering is an additional effect which influences the dielectric response. It implies that P_f is perpendicular to the tetragonal c-axis (like in Ca-doped crystals[22]). This supports the idea that the grain boundary dipole moment is not caused by random defects but rather by specific atomic arrangement.[34,35] Moreover it implies that the tetragonal phase develops in a specific fixed orientation with respect to the grain boundary structure, since P_f exists in the cubic phase prior to the structural transition. This calls for microstructural studies of the tetragonal phase in a bicrystal. We believe that also in thin STO films the appearance of polar regions, which causes coupling between the TO_1 and structural soft modes, is the important reason for a smaller softening of the former mode[8–11] and consequently lower permittivity.

Finally, let us briefly discuss the MW losses in STO ceramics. Our theoretical model cannot explain the increased losses compared to single crystals[2,3] using the soft mode response only. The model can account for the decrease in MW permittivity, but does not yield increase in losses. Whereas in good single crystals the two-phonon absorption seems to explain the whole MW losses at least above T_a,[39] in ceramics additional losses due to grain-boundary scattering proportionally to the one-phonon density of states may be activated. This yields additional losses proportional to frequency, which dominate in the higher GHz range,[2,40] whereas at lower frequencies also relaxational contributions proportional to $1/\omega$ were observed.[3,41] These losses, which point to charged point defects and/or fluctuations in the grain-boundary polarization P_f, have been not yet studied systematically. This needs wide-frequency and temperature studies on well defined samples, which are quite difficult to perform.

Acknowledgements

The work was supported by the Grant Agency of the Czech Republic (project Nos. 202/98/1282 and 202/00/1187) and Ministry of Education of the Czech Republic (COST-525).

References

1. Barker, A. S. and Tinkham, Jr., M., Far-infrared ferroelectric vibration mode in $SrTiO_3$. *Phys. Rev. B,* 1962, **125**, 1527–1530.
2. Rupprecht, G. and Bell, R. O., Microwave losses in strontium titanate above phase transition. *Phys. Rev. B,* 1962, **125**, 1915–1920.
3. Bethe, K., Über das Mikrowellenverhalten nichtlinearer Dielektrika. In *Philips Res. Repts. Suppl.*, Eindhoven, Centrex, 1970, No. 2, pp. 1–145.
4. Vendik, O. G., Hollmann, E. K., Kozyrev, A. B. and Prudan, A. M., Ferroelectric tuning of planar and bulk microwave devices. *J. Supercond.,* 1999, **12**, 325–338.
5. Christen, H.-M., Mannhart, J., Williams, E. J. and Gerber, Ch., Dielectric properties of sputtered $SrTiO_3$ films. *Phys. Rev. B,* 1994, **49**, 12095–12104.
6. Li, H.-C., Si, W., West, A. D. and Xi, X. X., Thickness dependence of dielectric loss in $SrTiO_3$ thin films. *Appl. Phys. Lett.,* 1998, **73**, 464–466.
7. Fuchs, D., Schneider, C. W., Schneider, R. and Rietschel, H., High dielectric constant and tunability of epitaxial $SrTiO_3$ thin film capacitors. *J. Appl. Phys.,* 1999, **85**, 7362–7369.
8. Fedorov, I., Železný, V., Petzelt, J., Trepakov, V., Jelínek, M., Trtík, V., Ćerňanský, M. and Studnička, V., Far-infrared specroscopy of a $SrTiO_3$ thin film. *Ferroelectrics,* 1998, **208-209**, 413–427.
9. Železný, V., Petzelt, J. and Kämmer, K., Infrared specroscopy of laser deposited $Ba_xSr_{1-x}TiO_3$ thin films. *J. Kor. Phys. Soc.,* 1998, **32**, S1615–S1617.
10. Petzelt, J., Ostapchuk, T., Kamba, S., Rychetský, I., Savinov, M., Volkov, A., Gorshunov, B., Pronin, A., Hoffmann, S., Waser, R. and Lindner, J., High-frequency dielectric response of $SrTiO_3$ crystals, ceramics and thin films. *Ferroelectrics,* 2000, **239**, 117–124.

11. Sirenko, A. A., Bernhard, C., Golnik, A., Clark, A. M., Hao, J., Si, W. and Xi, X. X., Soft-mode hardening in $SrTiO_3$ thin films. *Nature,* 2000, **404**, 373–376.
12. Hoffmann, S. and Waser, R., Curie–Weiss law of $(Ba_{1-x}Sr_x)TiO_3$ thin films prepared by chemical solution deposition. *J. Phys. IV France,* 1998, **8**, Pr9-221–Pr9-224.
13. Waser, R. and Lohse, O., Electrical characterization of ferroelectric, paraelectric, and superparaelectric thin films. *Integr. Ferroelectrics,* 1998, **21**, 27–40.
14. Streiffer, S. K., Basceri, C., Parker, C. P., Lash, S. E. and Kingon, A. I., Ferroelectricity in thin films: The dielectric response of fiber-textured $(Ba_xSr_{1-x})Ti_{1+y}O_{3+z}$ thin films grown by chemical vapor deposition. *J. Appl. Phys.,* 1999, **86**, 4565–4575.
15. Pertsev, N. A., Tagantsev, A. K. and Setter, N., Phase transitions and strain-induced ferroelectricity in $SrTiO_3$ epitaxial thin films. *Phys. Rev. B,* 2000, **61**, R825–R828.
16. Ryen, L., Olsson, E., Madsen, L. D., Wang, X., Edvardsson, C. N. L., Jacobsen, S. N., Helmersson, U., Rudner, S. and Wernlund, L.-D., Microstructure and microwave dielectric properties of epitaxial $SrTiO_3$ films on $LaAlO_3$ substrates. *J. Appl. Phys.,* 1998, **83**, 4884–4890.
17. Müller, K. A. and Burkard, H., $SrTiO_3$: an intrinsic quantum paraelectric below 4 K. *Phys. Rev. B,* 1979, **19**, 3593–3602.
18. Dec, J., Kleemann, W. and Westwanski, B., Scaling behaviour of strontium titanate. *J. Phys.: Condens. Matter,* 1999, **11**, L1–L6.
19. Petzelt, J., Ostapchuk, T., Gregora, I., Hoffman, S., Lindner, J., Rafaja, D., Kamba, S., Pokorný, J., Bovtun, V., Porokhonskyy, V., Savinov, M., Vaněk, P., Rychetský, I., Peřina, V. and Waser, R., Far infrared and Raman spectroscopy of ferroelectric soft mode in SrTiO3 thin films and ceramics. *Integr. Ferroelectrics*, 2001, **32**, 11–20.
20. Waser, R., Baiatu, T. and Härdtl, K.-H., dc Electrical degradation of perovskite-type titanates: I. Ceramics. *J. Am. Ceram. Soc.,* 1990, **73**, 1645–1653.
21. Bednorz, J. G. and Müller, K. A., $Sr_{1-x}Ca_xTiO_3$: an XY quantum ferroelectric with transition to randomness. *Phys. Rev. Lett.,* 1984, **52**, 2289–2292.
22. Kleemann, W., Albertini, A., Kuss, M. and Lindner, R., Optical detection of symmetry breaking on a nanosccale in $SrTiO_3$: Ca. *Ferroelectrics,* 1997, **203**, 57–74.
23. Hirota, K., Hill, J. P., Shapiro, S. M., Shirane, G. and Fujii, Y., Neutron- and *x*-ray-scattering study of the two lengthscales in the critical fluctuations of $SrTiO_3$. *Phys. Rev. B,* 1995, **52**, 13195–13205.
24. Wang, R., Zhu, Y. and Shapiro, S. M., Structural defects and the origin of the second length scale in $SrTiO_3$. *Phys. Rev. Lett.,* 1998, **80**, 2370–2373.
25. Gervais, F., High-temperature infrared reflectivity spectroscopy by scanning interferometry. In *Infrared and Millimeter Waves*, ed. K. J. Button. Academic Press, New York, 1983, pp. 279–339.
26. Nilsen, W. G. and Skinner, J. G., Raman spectrum of strontium titanate. *J. Chem. Phys.,* 1968, **48**, 2240–2248.
27. Fleury, P. A., Scott, J. F. and Worlock, J. M., Soft phonon modes and the 110 K phase transition in $SrTiO_3$. *Phys, Rev. Lett.,* 1968, **21**, 16–19.
28. Hayward, S. A. and Salje, E. K. H., Cubic-tetragonal phase transition in $SrTiO_3$ revisited: Landau theory and transition mechanism. *Phase Trans.,* 1999, **68**, 501–522.
29. Okai, B. and Yoshimoto, J., Pressure dependence of the structural phase transition temperature in $SrTiO_3$ and $KMnF_3$. *J. Phys. Soc. Jpn.,* 1975, **39**, 162–165.
30. Petzelt, J. and Dvořák, V., Changes of infrared and Raman spectra induced by structural phase transitions: II. Examples. *J. Phys. C: Solid State Phys.,* 1976, **9**, 1587–1601.
31. Itoh, M., Wang, R., Inaguma, Y., Yamaguchi, T., Shan, Y.-J. and Nakmura, T., Ferroelectricity induced by oxygen isotope exchange in strontium titanate perovskite. *Phys. Rev. Lett.,* 1999, **82**, 3540–3543.
32. Sirenko, A. A., Akimov, I. A., Fox, J. R., Clark, A. M., Li, H.-C. H., Si, W. and Xi, X. X., Observation of the first-order Raman scattering in $SrTiO_3$ thin films. *Phys. Rev. Lett.,* 1999, **82**, 4500–4503.
33. Uwe, H., Yamaguchi, H. and Sakudo, T., Ferrolectric microregion in $KTa_{1-x}Nb_xO_3$ and $SrTiO_3$. *Ferroelectrics,* 1989, **96**, 123–126.
34. McGibbon, M. M., Browning, N. D., McGibbon, A. J. and Pennycook, S. J., The atomic structure of asymmetric tilt boundaries in $SrTiO_3$. *Phil. Mag. A,* 1996, **73**, 625–641.
35. Browning, N. D., Moltaji, H. O. and Buban, J. P., Investigation of three-dimensional grain-boundary structures in oxides through multiple-scattering analysis of spatially resolved electron-energy-loss spectra. *Phys. Rev. B,* 1998, **58**, 8289–8300.
36. Rychetský, I. and Hudák, O., Ferroelectric phase transition in small spherical particles. *J. Phys. Cond. Matter,* 1997, **9**, 4955–4965.
37. Frey, M. H., Xu, Z., Han, P. and Payne, D. A., The role of interfaces on an apparent grain size effect on the dielectric properties for ferroelectric barium titanete ceramics. *Ferroelectrics,* 1998, **206-207**, 337–353.
38. Yamanaka, A., Kataoka, M., Inaba, Y., Inoue, K., Hehlen, B. and Courtens, E., Evidence for competing orderings in strontium titanate from hyper-Raman scattering spectroscopy. *Europhys. Lett.,* 2000, **50**, 688–694.
39. Tagantsev, A. K., About dielectric loss in displacive type ferroelectrics. *Zh. Eksp. Teor. Fiz.,* 1984, **86**, 2215–2228 (in Russian).
40. Silverman, B. D., Microwave absorption in cubic strontium titanate. *Phys. Rev.,* 1962, **125**, 1921–1930.
41. Buzin, I. M., High-frequency dielectric loss of strontium titanate. *Vestn. Mosk. Univ.,* 1977, **18**, 70–76 (in Russian).